

## Supporting Information

# Direct Observation of Structural Properties and Fluorescent Trapping Sites in Macrocyclic Porphyrin Arrays at the Single-Molecule Level

Sujin Ham,<sup>a</sup> Ji-Eun Lee,<sup>a</sup> Suhwan Song,<sup>a</sup> Xiaobin Peng,<sup>b</sup> Takaaki Hori,<sup>b</sup> Naoki Aratani,<sup>b</sup> Atsuhiko  
Osuka,<sup>\*b</sup> Eunji Sim,<sup>\*b</sup> and Dongho Kim<sup>\*a</sup>

<sup>a</sup>Department of Chemistry, Yonsei University, 50, Yonsei-ro, Seodaemun-gu, Seoul, 120-749, Korea

<sup>b</sup>Department of Chemistry, Graduate School of Science, Kyoto University, Sakyo-ku, Kyoto, 606-8502,  
Japan

### Corresponding Authors

[dongho@yonsei.ac.kr](mailto:dongho@yonsei.ac.kr) (D. Kim); [esim@yonsei.ac.kr](mailto:esim@yonsei.ac.kr) (E. Sim), and [osuka@kuchem.kyoto-u.ac.jp](mailto:osuka@kuchem.kyoto-u.ac.jp) (A. Osuka)

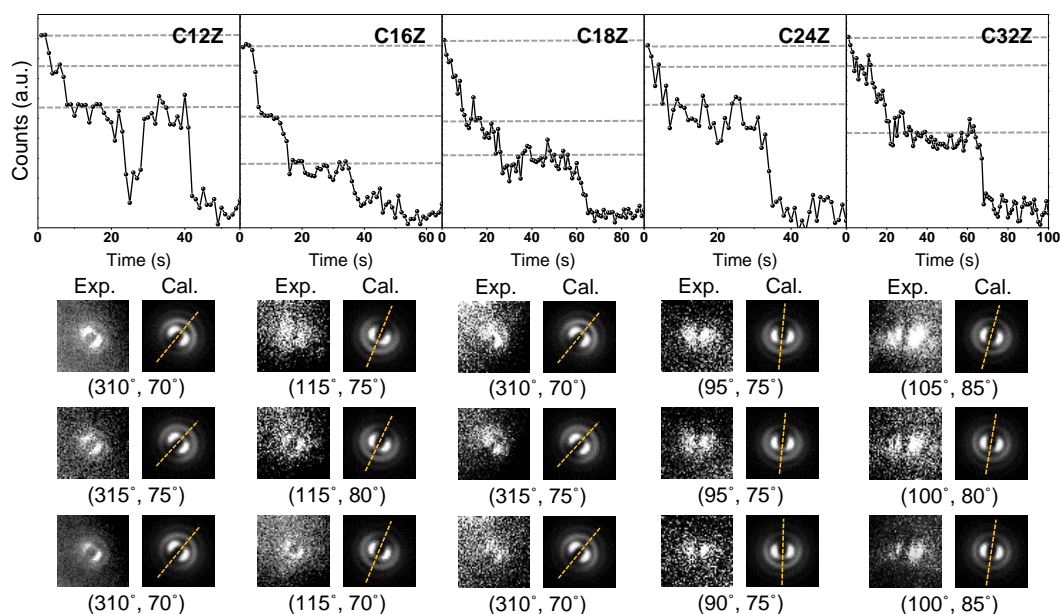


**Fig. S1** Representative fluorescence intensity trajectories (FITs) along with defocused images of **C12Z**, **C16Z**, **C18Z**, **C24Z**, and **C32Z**. Fluorescence intensity trajectories reconstructed from consecutive defocused images obtained for a single molecule with a bin time of 1 s. Defocused images on the left are experimentally observed images and the corresponding calculated images are on the right. On the basis of calculated in-plane ( $\phi$ ) and out-of-plane ( $\theta$ ) angles, the molecular orientation can be displayed as vector components using polar coordinate.

These representative examples show only one emission pattern despite multi-step photobleaching behavior in the fluorescence intensity trajectories (FITs). The defined dipole orientations ( $\phi$ ,  $\theta$ ) of the first, second, and third intensity levels for the **C12Z** molecule are (310°, 70°), (315°, 75°), and (310°, 70°), respectively. Similar patterns were also observed for **C16Z**, **C18Z**, **C24Z** and **C32Z** molecules. Since the excitation energy transfer process between **Z2** units allows for preferential emission from the chromophore in the lowest energy state, the orientations of emission patterns in each step are the same. Our results demonstrate that cyclic porphyrin systems are suitable for efficient light harvesting complexes comprising many light-absorbing units.

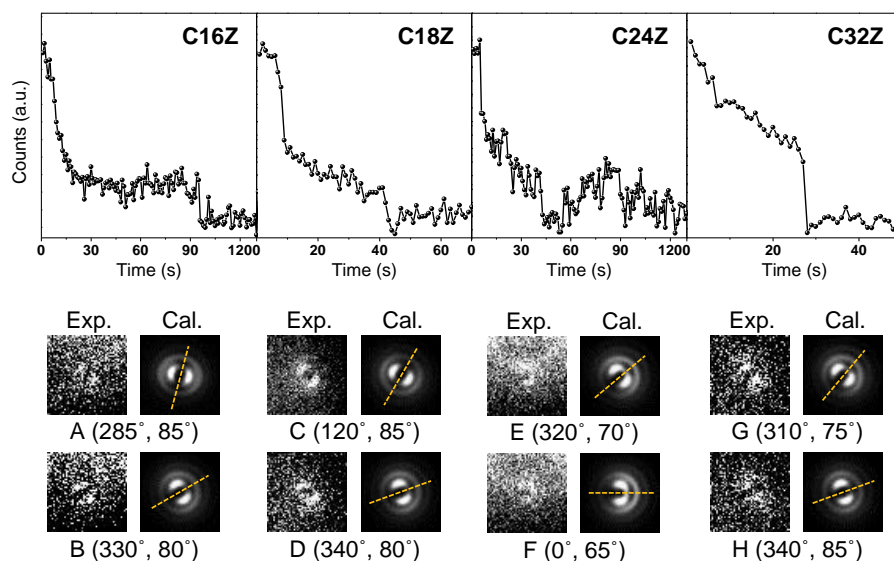


**Fig. S2** Representative fluorescence intensity trajectories (FITs) along with defocused images of **C16Z**, **C18Z**, **C24Z**, and **C32Z**. FITs are plotted as the integrated intensity of each defocused image with a bin time of 1 s. Defocused images on the left are experimental images, and the corresponding simulated images are on the right. On the basis of calculated in-plane ( $\phi$ ) and out-of-plane ( $\theta$ ) angles, the molecular orientation can be displayed as vector components using polar coordinate.

For the **C16Z** molecule, the defined dipole orientations ( $\phi$ ,  $\theta$ ) were A (285°, 85°) and B (330°, 80°). We calculated the interchromophoric angles using the law of cosines after converting spherical coordinate to Cartesian coordinates;  $\angle AB$  is 44.9°, which is in excellent agreement with the value of 45° expected from a the two-dimensional octagonal structure. Similarly, we calculated the interchromophoric angles of the **C18Z**, **C24Z**, and **C32Z** molecules;  $\angle CD$ ,  $\angle EF$ , and  $\angle GH$  are 42.6°, 37.2°, and 31.1°, respectively. All interchromophoric angles in Figure S2 are in good agreement with the values of interchromophoric angles from the two-dimensional polygonal structure.

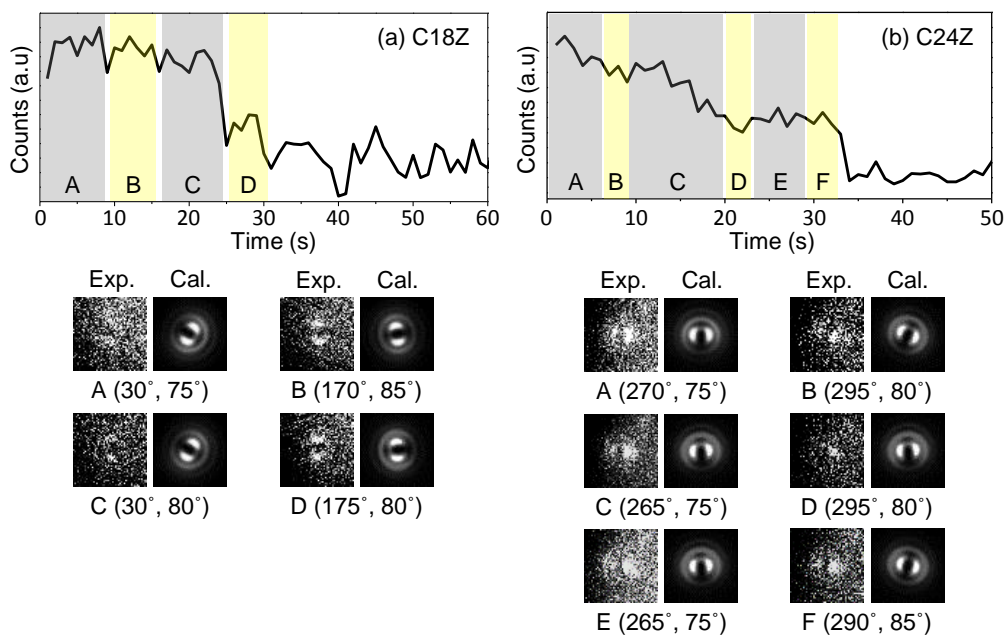


**Fig. S3** Representative fluorescence intensity trajectories (FITs) and corresponding defocused images of (a) **C18Z** and (b) **C24Z** molecules whose fluorescence was alternately emitted from two chromophores. FITs are plotted as the integrated intensity of each defocused image with a bin time of 1 s. Defocused images on the left are experimental images, and the corresponding simulated images are on the right. On the basis of calculated in-plane ( $\phi$ ) and out-of-plane ( $\theta$ ) angles, the molecular orientation can be represented as vector components using polar coordinate.

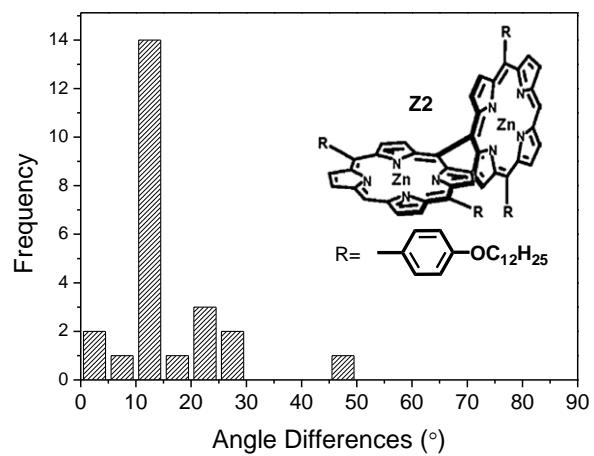


**Fig. S4** Histogram of the angle differences of **Z2** units which shows little movement in the polymeric matrix environment (30%). 70% of the **Z2** molecules showed no movements.

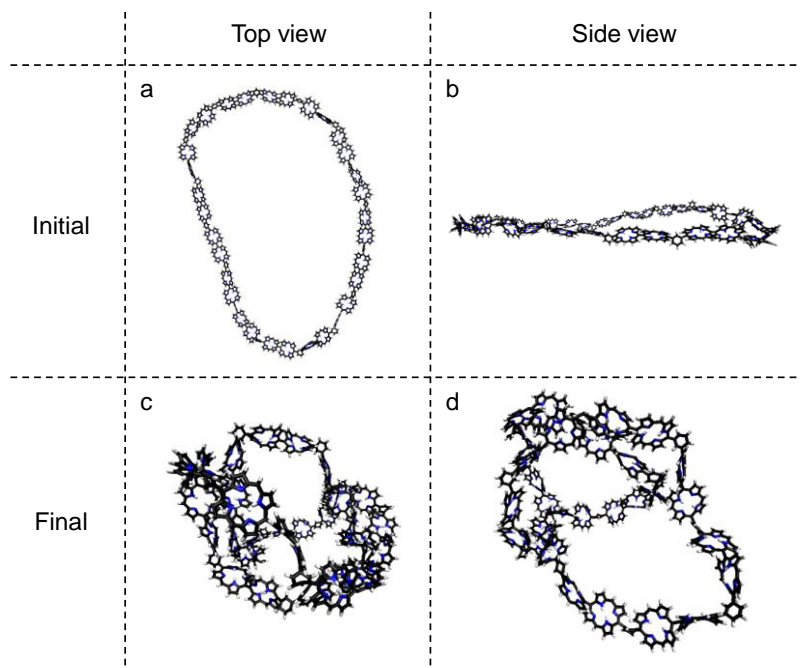


**Fig. S5** Sketch of optimized structures of **C32Z**. (a) top view and (b) side view of the initial state, and (c) top view and (d) side view of the final state. As shown in the final structures, **C32Z** has a completely distorted structure due to the extremely large molecular structure.

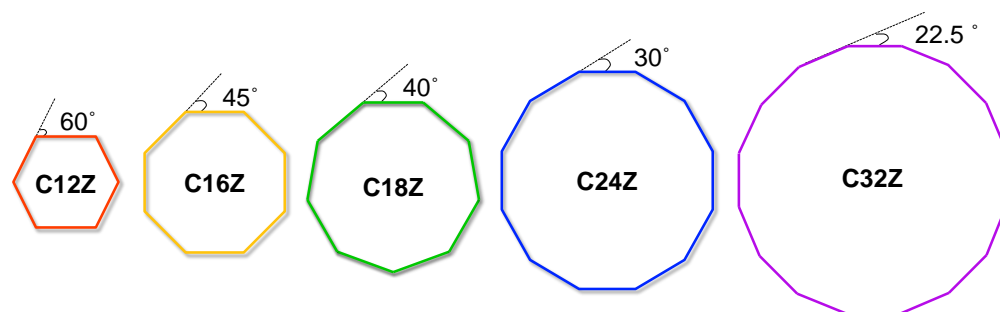


**Fig. S6** Two-dimensional regular polygon model in which all meso-carbons of the porphyrins lie in the same plane.

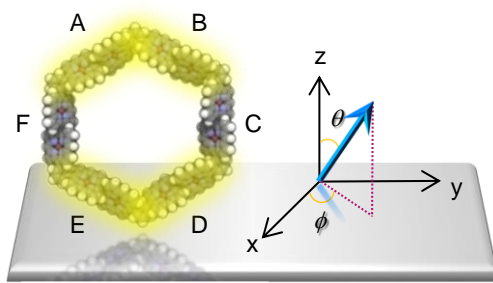


**Fig. S7** Schematic representation of the influence of orientation of the units.

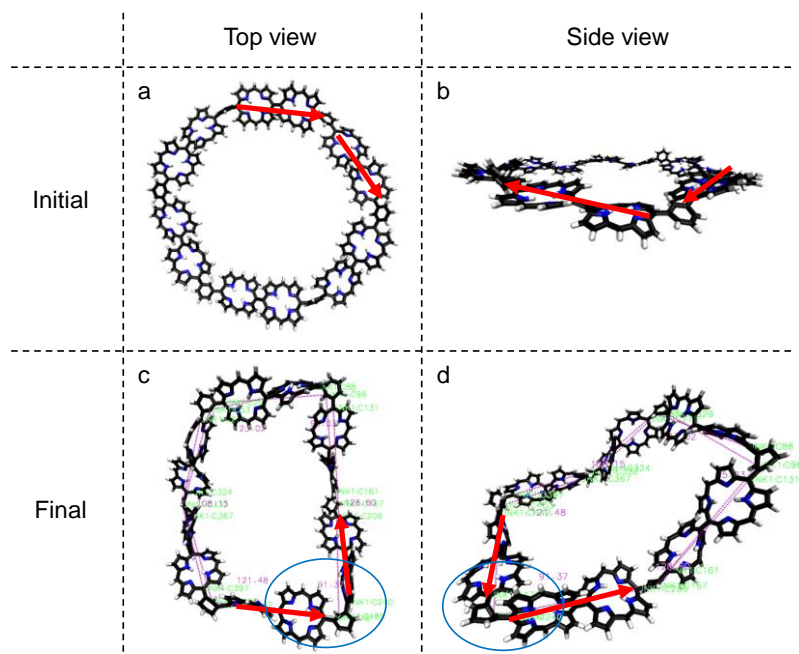


**Fig. S8** Sketch of optimized structures of **C12Z**. (a) top view and (b) side view of the initial state, and (c) top view and (d) side view of the final state. There are many occurrences in the large angle region due to the larger degrees of freedom in the simulated conditions.

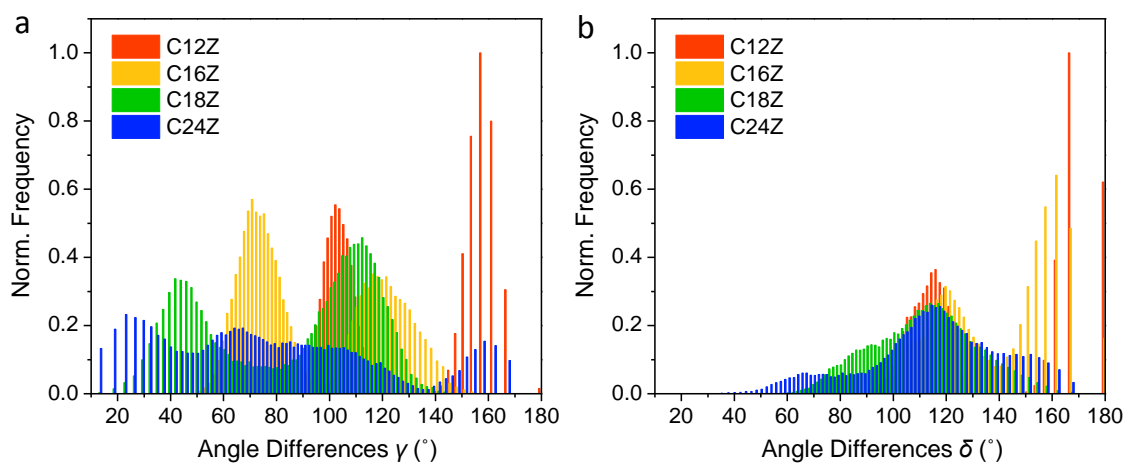


**Fig. S9** Distribution of interchromophoric angles, (a)  $\gamma$  and (b)  $\delta$  in Scheme 1, calculated from 6,000 conformations generated by MD simulations.

**Table S1.** Summary of parameters for angle differences of **CNZs**.

	Experimental value $\alpha$ (°)		Simulated value $\beta$ (°)		Theoretical Value <sup>e</sup> (°)
	M <sup>a</sup>	FWHM <sup>b</sup>	M <sup>c</sup>	FWHM <sup>d</sup>	
<b>C12Z</b>	56.7	15.8	67.1, 86.2	14.0	60
<b>C16Z</b>	41.6	20.0	55.8	40.3	45
<b>C18Z</b>	38.0	27.3	54.4	42.2	40
<b>C24Z</b>	37.2	25.1	48.5	43.2	30
<b>C32Z</b>	32.5	25.5			22.5

<sup>a</sup>The center of the Gaussian fit of experimentally obtained histograms. <sup>b</sup>The full width at half-maximum values of experimentally obtained histograms. <sup>c</sup>The center of the Gaussian fit of computationally obtained histograms. <sup>d</sup>The full width at half-maximum values of computational obtained histograms. <sup>e</sup>The adjacent angles of two-dimensional regular polygon model of **CNZs** (Fig. S6).